Climatology of Cyclones and Their Tracking over Southern Coasts of Caspian Sea

Molanejad M.[1,2*], Soltani M.[3], Ranjbar SaadatAbadi, A.[4], Babu C. A.[5], Sohrabi M.[6] and Martin M. V.[7]

[1]Iranian Research Organization for Science and Technology (IROST), Tehran, Iran

[2]IORA- Regional Center for Science and Technology Transfer, Tehran, Iran

[3]Department of Physical Geography, Faculty of Geography, University of Tehran, Iran

[4]Atmospheric Sciences and Meteorological Research Center (ASMERC) of I. R. of Iran Meteorological Organization (IRIMO), Tehran, Iran

[5]Department of Atmospheric Sciences, Cochin University of Science and Technology, Cochin 682 016, India

[6]Department of Biological and Agricultural Engineering, University of Idaho, Boise, ID 83702, USA

[7]Centre for Oceans, Rivers, Atmosphere and Land Sciences (CORAL), Indian Institute of Technology, Kharagpur, India

ABSTRACT: The southern coasts of Caspian Sea is subjected to synoptic/mesoscale weather systems ranging from locally enhanced sea breeze formation and small local front systems to synoptic scale cyclones. This study presents climatology of cyclones over the southern coasts of Caspian Sea covering a ten year period 1996-2005. Altogether 57 cyclones were formed during the ten year period. A noticeable seasonality is observed in evolution of cyclones over the entire Caspian region, a majority of the 57 cyclones (73.7%) were developed during winter and fall seasons while the remaining (26.3%) occurred during spring and summer seasons. Most of the cyclones were of low intensity, out of 57 cyclones observed during the ten year period 16 (28%) were deep depressions and 24 (42.1%) were cyclonic storms. Altogether 5 super cyclonic storms were observed during the period, out of which 4 were observed during winter and fall seasons. Mid-tropospheric, large-scale processes and local features were responsible for the initial development of all weather systems. The Mediterranean Sea plays a significant role in cyclogenesis and propagation of the systems the Caspian region. Further, a Mediterranean cyclonic system formed during October 2001 was studied in detail using backward trajectory *Lagrangian model: Hybrid Single Particle Lagrangian Integrated Trajectory* (HYSPLIT). The HYSPLIT model outputs confirmed the observed synoptic features for the weather system of the case study.

Key words: High-pressure systems, Mid-latitude cyclones, Moisture convergence, HYSPLIT, Tracking, north of Iran

INTRODUCTION

Southern coasts of Caspian Sea i.e. a distance between the Alborz mountain range and Caspian Sea itself, is considered as the smallest climatic area of Iran (Alijani, 1997). The Caspian Sea as the world's largest lake plays a significant role in the climate of the northern areas of Iran. A location map together with 5-stations including Bandar-e-Anzali, Rasht, Ramsar, Sari and Gorgan is shown in figure 1 and the geographical characteristics of the stations are presented in Table 1. It is often subject to synoptic and mesoscale weather systems that threaten life and property at sea or on the coast. These systems range from locally

enhanced sea breeze formation (Khoshhal, 1997) and small local front systems near the southern coasts (Khalili, 1971), to synoptic scale trough and westerly cyclone (Moradi, 2001, 2004, 2006). They, however, vary in intensity and structure across a spectrum that includes both weak and intense cold-cored systems from Siberian high to warm-cored mid-latitude cyclones called as westerly systems. Westerly systems are so named particularly in autumn season, because subtropical cyclones can have warm-cored centers with spiral convective rain bands over the southern coasts of Caspian Sea. In this study we concentrate on cyclones in Caspian Sea that threaten life and property as a result of heavy coastal rain

*Corresponding author E-mail: mmolanezhad@yahoo.com
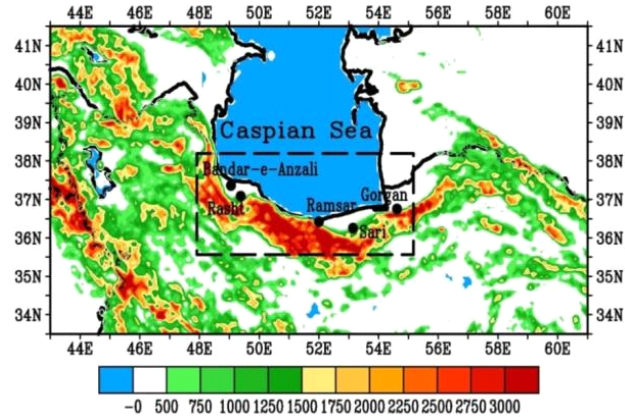
Fig.1. Map of the southern Caspian Sea and surrounding region with the underlying topography in meters. The study area is enclosed by the black dashed rectangle with the five weather stations

Table 1. Geographical characteristics of the selected weather stations in the Caspian region

No.	Station Name	Latitude (N)	Longitude (E)	Elevation (m)
1	Bandar-e-Anzali	37°28′	48°28′	-26.2
2	Rasht	37°12′	49°39′	36.7
3	Ramsar	36°54′	50°40′	-20
4	Sari	36°33′	53°00′	23
5	Gorgan	36°51′	54°16′	13.3

(above 50 mm) or the combined effects of wind and sea state. A ten-year climatology of Caspian Sea cyclones from 1996 to 2005 in five weather stations, reveals a range of the heavy rainfall events over the region. The study has three objectives. The main objective is to present a climatology of southern Caspian Sea cyclonic systems and mapping their tracks over the area north of 35.5° N, south of 38.5° N, west of 55°E and east of 48° E for the period 1996 to 2005. The next objective is to study the Westerly high-pressure system of October 2001, on the basis of a synoptic analysis of life cycle of this particular storm from its beginning as a weak high in the Caspian Sea, to its landfall and a heavy rainfall event over land. The third objective is to bring out the backward trajectories on the mid-latitude cyclone, employing the *Hybrid-Single Particle Lagrangian Integrated Trajectory* (HYSPLIT) model, which was developed by NOAA ARL.

Zishka and Smith (1980) examined storm tracks during January and July and demonstrated an equatorward shift of the storm track in January relative to July, with principal areas of cyclogenesis in the lee of the Rocky Mountains and along the U.S. east coast. Whittaker and Horn (1981) also found a decreasing trend in the frequency of storms for this period in North America, but no significant trend was evident for the *Northern Hemisphere* (NH). Trends in cyclone frequency in the NH for 1958-97 were examined at the 1000 and 500 hPa levels by Key and Chan (1999), using the NCEP/NCAR reanalysis. They showed that for 60°–90°N, closed lows increased in frequency at 1000 hPa in all seasons, but they decreased in frequency at 500 hPa except in winter. In mid-latitudes, the frequency of lows decreased at 1000 hPa but increased at 500 hPa, except in winter. For 0Ú″30ÚN, lows became more frequent at both levels in winter and spring and at 500 hPa only in summer and autumn. The spatial distribution of systems identified by Serreze *et al.* (1993) and Serreze (1995) during 1973-92, showed that in winter months, the most of the cyclones near Iceland extends northeastward into the Norwegian-Barents Sea. In the summer half year, this tendency is almost absent. In winter the rate of cyclones deepening and the frequency of deepening events peak in the area of the Icelandic low, southwest of Iceland, with a separate maximum in the Norwegian Sea (Serreze *et al.,* 1997).

Cyclogenesis is common in these areas, as well as in northern Baffin Bay. Deepening rates are up to "6.8 hPa (12 h-1 d) for the Greenland Sea – North Atlantic sector. The combined effects of ice-edge baroclinicity, orographic forcing, and rapid boundary layer modification in off-ice airflows are probably involved. Additionally, the same locations show high frequencies active one with alternating regimes. Objective climatology of cyclones in the Mediterranean region was performed by Trigo *et al.,*

Table 2 Climatology of cyclones formed in the southern coasts of Caspian Sea that resulted in heavy rainfall (more than 50 mm) during 1996-2005 in different months covering the area north of 36° N, south of 38° N, west of 55° E and east of 48° E, in five weather stations.

Weather Stations	Jan.	Feb.	Mar.	Apr.	May	June	July	Aug.	Sept.	Oct.	Nov.	Dec.
Bandar-e-Anzali	1	1						1	9	5	3	4
Rasht		2		1					2	3	4	2
Babolsar			1						1	3	4	1
Sari		1	1	1					1		1	
Gorgan	1	2										1
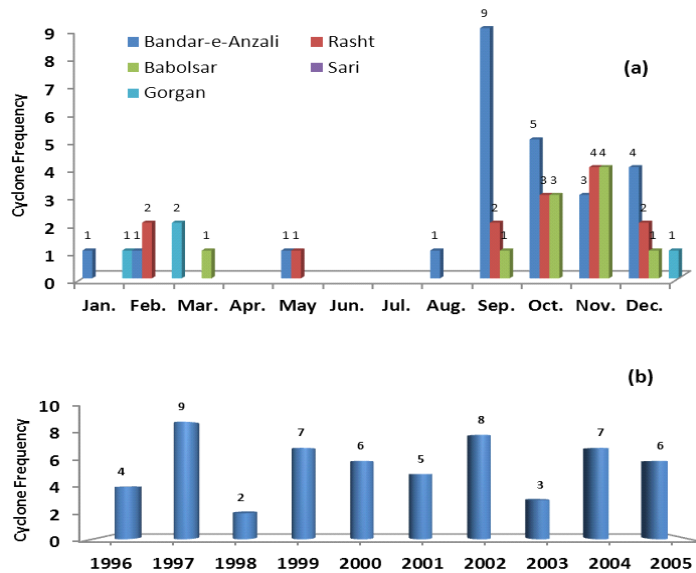
Fig. 2. Frequency of occurrence of cyclones: (a) monthly frequency for individual stations, (b) annual frequency over the five stations together in the southern coasts of Caspian Sea

(1999). They found that the regions where cyclogenesis is mainly controlled by topography, like the Gulf of Genoa and south of the Atlas Mountains, seem to generally account for the most intense events. Hobbs *et al.* (1990, 1996) re-examined the structure of cyclones in the central United States and proposed a new conceptual model. Their conceptual model featured a warm-sector precipitation band that was caused by frontogenesis at midlevels, a feature they termed a cold front aloft. In presenting this conceptual model, Hobbs et al. (1996) re-analyzed the cyclone discussed by Rossby and Weightman (1926). Each of the features in the Rossby and Weightman (1926) cyclone was related to and compared to a similar feature in the Hobbs et al. (1996) model except for W1, which Hobbs et al. (1996) did not consider a significant feature. Blender *et al.* (1997), by using the 5-yr European Centre for Medium-Range Weather Forecasts analysis from 1990 to 1994 with a 6-h

interval and T106 horizontal resolution, identified the cyclone-track regimes in the North Atlantic. As far as we know, there is no document to demonstrate studies on climatology of cyclonic systems and their tracking over southern coasts of Caspian Sea. Therefore, an attempt is made to carry out analysis on cyclone climatology in the region. Climatology of cyclones over the southern Caspian Sea during the period as of January 1996 to December 2005 was studied by identifying systems with at least one closed pressure contour on SLP charts covering the region north of 36°N, south of 38°N, east of 48°E and west of 55°E. The criterion for the inclusion of these systems was made by identifying those that produced at least 10 times the monthly mean daily rainfall at a few of the southern Caspian Sea coastal synoptic reporting stations. The rainfall threshold was determined as 50 mm in establishing the climatology of southern Caspian Sea coasts high-pressure systems.
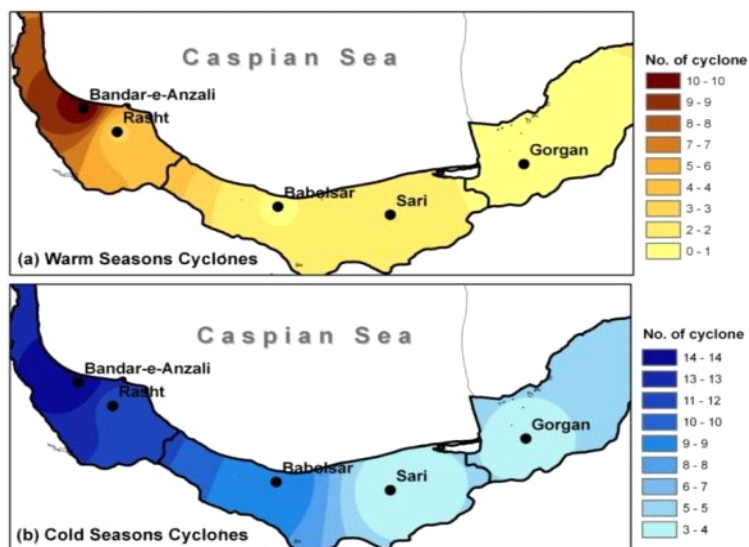
Fig. 3. Interpolation of cyclone frequencies in (a) warm season and (b) cold season during a ten-year period from 1996 through 2005 over the southern coasts of Caspian Sea – warm season in Iran starts from April through September and cold season begins from October through March.
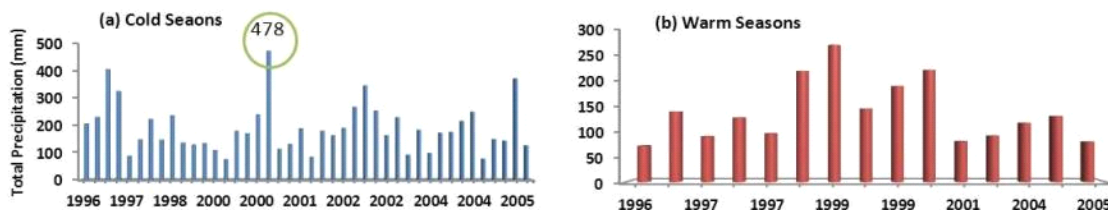
Fig. 4. Time series of accumulated precipitation (mm) for five stations caused by 57 cyclone events *i.e.* 42 in cold season (a) and 15 in warm season (b) over southern coasts of Caspian Sea. The green circle in (a) indicates the storm of October 1, 2011, which was identified as the severest storm during the study period, and discussed as a case study in section 3.1.

57 systems formed during the ten-year period in the region with the five stations along the Caspian region (see Table 1). In the Caspian region, the maximum rainfall occurrence was identified in the farthest point of the southwest Caspian Sea, where Bandar-e-Anzali is located, resulting from the formation of a local front in times of extending the Northerly winds over the SefidRood valley (Khalili, 1971), or formation of a front so-called sea breeze front between the sea and land (Khoshhal, 1997) is another mechanism which was stated for maximum rainfall occurrence over the southern coasts of Caspian Sea. According to table 1, stations located in the west of the Caspian region *i.e.* Bandar-e-Anzali and Rasht, received high amount of rainfall during late summer and early autumn seasons. On the contrary, the eastern stations *i.e.* Sari and Gorgan in the Caspian region received highest rainfall during winter season. Therefore, the number of cyclones formed over the west Caspian region is much more than those occurred in the

eastern region. This fact is clearly presented in figure 3, which indicates the spatial distribution of cyclone frequencies in warm and cold seasons during the study period over the southern coasts of Caspian Sea. A huge number of cyclones, as figure 3 indicates, both in warm and cold seasons occur in the west of the region and gradually dwindles toward the eastern areas. The temporal distribution of the cyclone occurrence on an annual basis is also illustrated in Fig. 2b. Based on figure 2b, the most frequent cyclone event occurred in the year 1977 with 9 storms, while the lowest one took place in the year 1998 with only 2 storms. On the whole, the frequency of cyclone occurrence indicates a year-to-year fluctuation; nevertheless it shows a slightly ascending trend over the region (Fig. 2b). It is believed that, however, the convection event plays a significant role in the occurrence of autumn heavy precipitations over the Caspian region (Khalili, 1971; Alijani, 1993; Afshar Moghadam, 1994; Ghashghaei, 1996). Meanwhile,

120
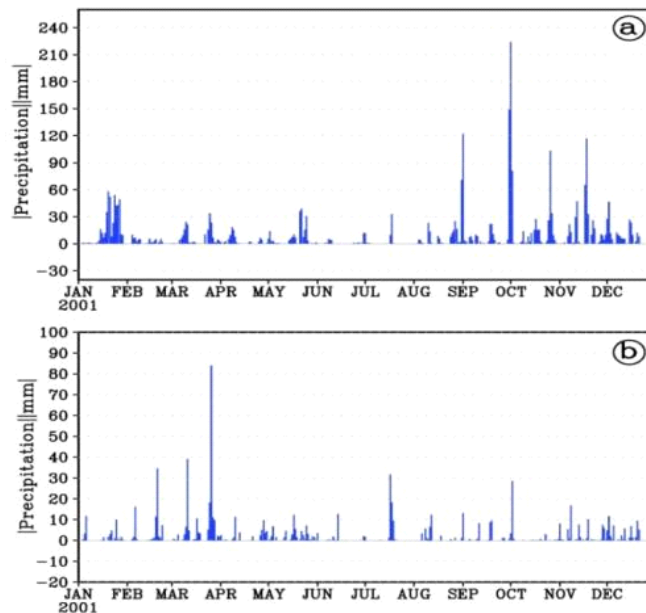
Fig. 5. Time series of daily total precipitation (mm) for (a) Bandar-e-Anzali station (west of Caspian region) at latitude 37.5°N and longitude 48.5°E. (b) Gorgan station (east of Caspian region) at latitude 37°N and longitude 55°E, both for a period of January 1, through December 31, 2001.

other research results indicate that eastward propagation of the Westerly immigrant high-pressure systems located over the Caspian region are responsible for the autumn rainfalls over the region (Bagheri, 1993; Vahidi, 1997; Khoshhal, 1997; Alijani, 2001; Yousefi, 2003; PourAtashi, 2005; Alijani *et. al.* 2007; Raziei *et. al.* 2008; JanbazGhobadi *et. al.* 2001).

Time series of the accumulated precipitation of five stations caused by 57 cyclone events in cold and warm seasons over southern coasts of Caspian Sea is shown in Fig. 4. It can be seen that the accumulated precipitation in five stations in cold season is almost twice as that in warm season, which indicates that not only the frequency of cyclone events in the cold season (42) is far more than that in warm season (15), but also the intensity of storms is more in cold season over the region. The green circle in (a) indicates the accumulated precipitation for the storm of October 1, 2011. This value is recognized as the highest amount of accumulated rainfall in five stations *i.e.* Bandar-e-Anzali (220), Rasht (154), Babolsar (55), Sari (39) and Gorgan (10) in millimeter. Further details about the event are discussed later as a case study in section 3.1. It is also worthwhile to mention that in both seasons there is a periodic fluctuation *e.g.* a 3-4 year cycles.

Additionally, figure 5 indicates the time series of total precipitation in Bandar-e-Anzali (Fig. 5a) and Gorgan (Fig. 5b) as a representative for the west and east of the Caspian region respectively, for the year

2001 just as a sample for the study period. Generally, the precipitation amount in the eastern stations is less than stations in the western region (by one third amount) (Fig. 5), which means that the total precipitation decreases gradually from west to the east of Caspian region. However, the case study presented here is for October 2001 high-pressure system, because the rainfall produced over the coastal areas during the event also resulted in flooding of southwestern coastal region of Caspian Sea. The town of Bandar-e-Anzali, which is located adjacent to the Caspian Sea in Gilan province, where the system made landfall, received heavy rainfall of 220 mm in the 24-h period on October 1, 2001 (Fig. 7a).

MATERIALS & METHODS

In order to examine the selected storm (cyclone) over the southern coasts of Caspian Sea synoptically, different data sources *i.e. National Centers for Environmental Prediction/National Center for Atmospheric Research* (NCEP/NCAR) reanalysis data (Kalnay *et al.*, 1996), the *European Centre for Medium-Range Weather Forecasts* (ECMWF), *Highly-Resolved Observational Data Integration Towards Evaluation of the Water Resources* (APHRODITE), and *National Oceanic and Atmospheric Administration – Air Resources Laboratory* (NOAA–ARL) ranging from hourly to daily variables at multiple levels of the atmosphere was utilized. In synoptic analysis, however, we considered the following variables: surface and

Table 2. Details of different data sets used for the cyclone under study in October 2001

Data Sources	Variables/Model	Units	Temporal Coverage	Spatial Coverage	Levels
NCEP/NCAR	geopotential height	m	4-times daily and daily	2.5 x 2.5 degree grid	multiple level
	precipitable water	Kg/m^{-2}	4-times daily	"	surface
	relative humidity	%	"	"	"
	sea surface pressure (SLP)	hPa	"	"	"
	u and v wind components	m/s^{-1}	"	"	"
	air temperature	^{o}C	"	"	"
	relative vorticity	10^{-5} s^{-1}	"	"	"
	moisture convergence*	g/kg^{-1} s^{-1}	hourly	"	"
ECMWF	Convective Available Potential Energy (CAPE)	J/kg^{-1}	"	0.5x0.5 degree grid	"
	total of precipitation	mm	"		"
APHRODITE	total of precipitation	mm	daily	0.25x0.25-degree grid	"
NOAA ARL	HYSPLIT backward trajectory	AGL	hourly	360 x 180 at 1 degree	multiple level
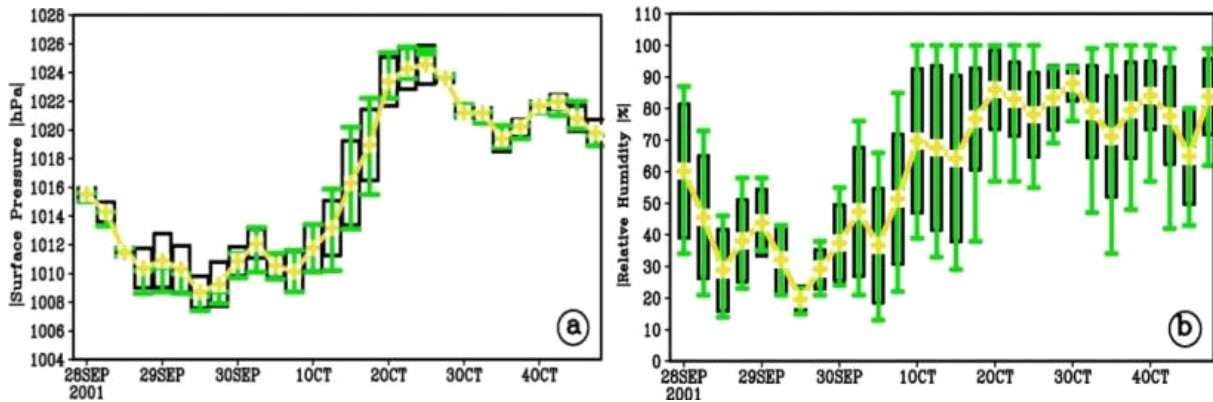
Fig. 6. Box and whisker plot: (a) demonstrates median (yellow line), lower and upper quartiles (black boxes), lower and upper extreme values (green bars) calculated to draw hourly surface pressure (6-hour time steps) over the area north of 36ºN, south of 38ºN, east of 48ºE, and west of 55ºE. (b) same as a, but for relative humidity variable

upper pressure levels, relative humidity, zonal and meridional wind components, convective available potential energy, precipitable water, and hourly and daily total precipitation. The meteorological charts then produced using *Grid Analysis and Display System* (GrADS) software. Additionally, the HYSPLIT (*Hybrid-Single Particle Lagrangian Integrated Trajectory*) model, developed by NOAA ARL, was used to compute the backward trajectories discussed in this study (Draxler and Rolph 2011; Rolph 2011). Each backward trajectory was computed for 48 hour duration with three ending levels (500, 1500 and 5000 m above ground level). The meteorological input for the trajectory model was the reanalysis dataset. HYSPLIT uses archived 3-dimensional meteorological fields generated from observations and short-term forecasts

(Stunder, 1997). Furthermore, the hourly and daily precipitation data used for the selected cyclone, gathered from ECMWF and APHRODITE's water resources project (Yatagai *et al.*, 2009), respectively. Details of the data sets used for the analysis is shown in Table 2.

RESULTS & DISCUSSION

In early October 2001, a high-pressure system (at surface level) approached the southern coasts of Caspian Sea at approximately latitude 36ÚN. It made landfall early on October 1 as an anticyclonic system mostly over the southwestern portion of the Caspian Sea southern coasts. Box and whisker plot of Sea Level Pressure (SLP) and relative humidity are shown in figure-3. A box and whisker plot, by
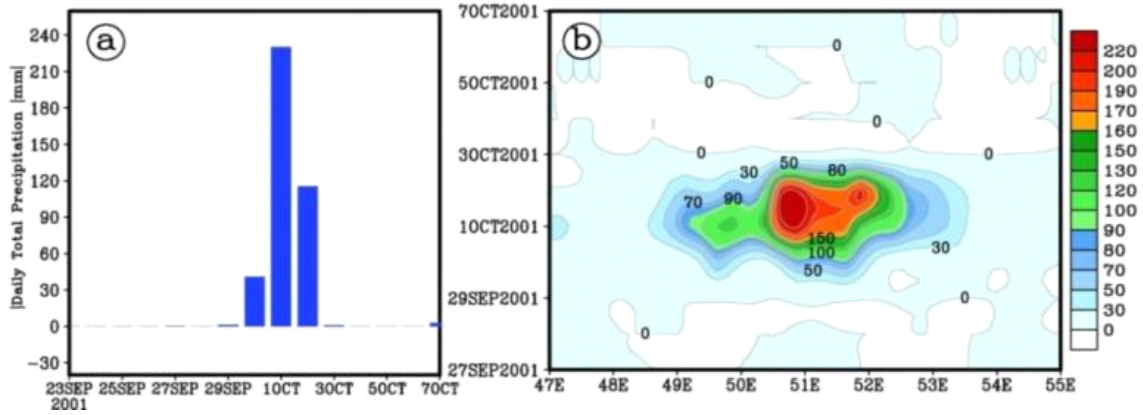
Fig. 7. (a) Indicates bar-chart of the time series of daily total of precipitation (mm) in Bandar-e-Anzali station (37.5ÚN, 49ÚE) and (b) shows time series of areal average precipitation over 37ÚN for the entire region
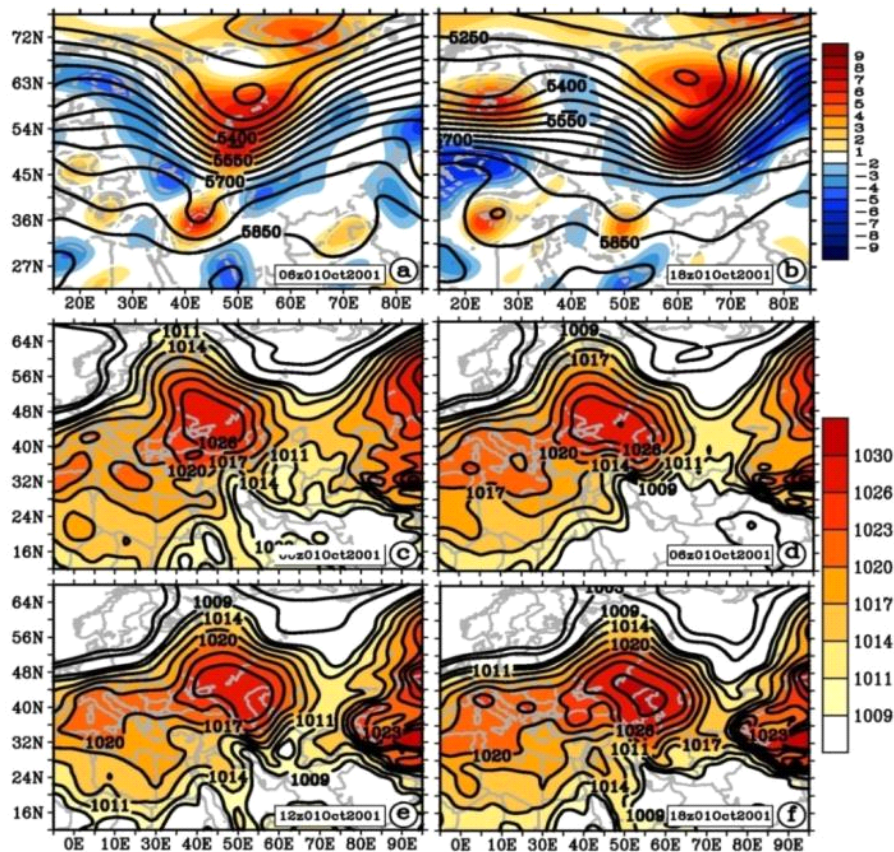
Fig. 8. Analysis charts derived from NCEP/NCAR reanalysis dataset for: 500 hPa geopotential height contours (m) and relative vorticity (10⁻⁵s⁻¹) shading in 6-hour time steps (a) 0600 UTC and (b) 1800 UTC October 1, 2001. The hourly SLP in hectopascal pressure (contours and shading) derived at 0000 UTC (c), 0600 UTC (d), 1200 UTC (e) and 1800 UTC October 1, 2001.

definition, is used to display the distribution of a single variable, and consists of a rectangle with a line extending from the center of each end, drawn next to a linear scale. The length of the box corresponds to the center of the data, from the first quartile to the third quartile. There is also a line dividing the box into two parts, drawn at the location of the median. The "whiskers" extend outward to the smallest and largest data values (Sanders, 2001). As it can be seen from the plot, SLP and relative humidity values
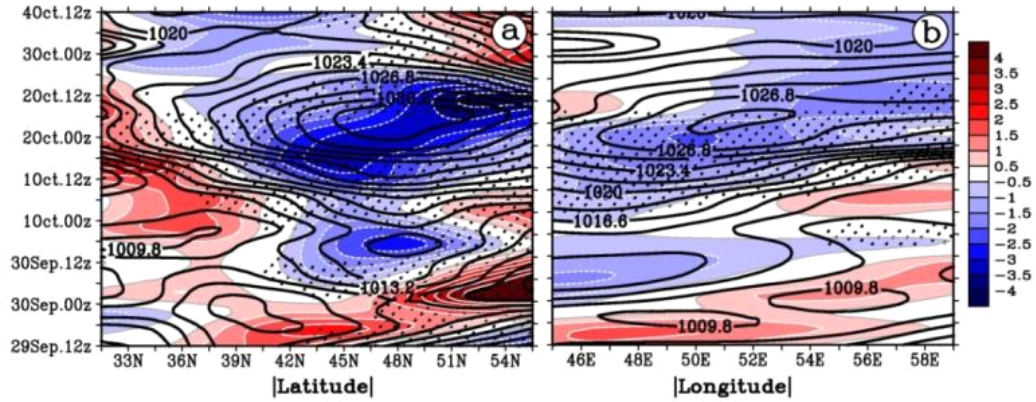
Fig.9. Hovmoller diagram of relative vorticity (10^{-5} s^{-1}) at 925 Hectopascal and sea level pressure (hPa) along: (a) longitude 49°E and (b) latitude 37°N. Hatched areas show wind velocity (magnitude) greater than 10 m s^{-1}.
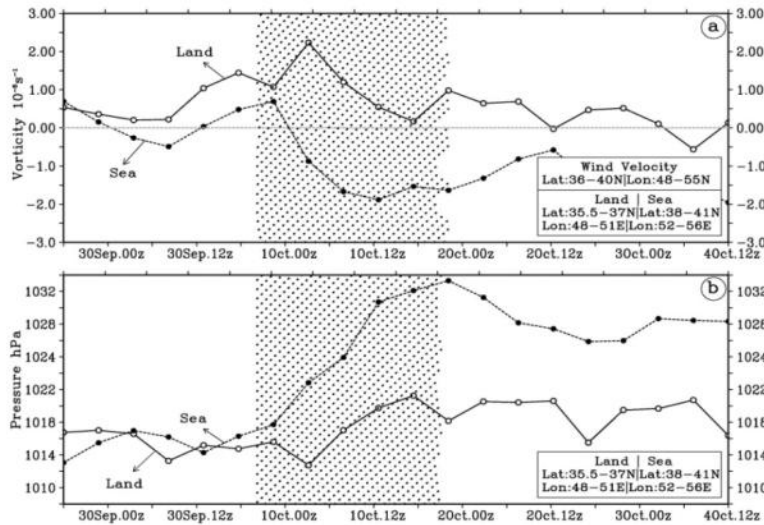
Fig. 10. Line graphs of relative vorticity (10^{-5} s^{-1}) (a) and sea level pressure (b) in land (solid line) and sea (dash line) over the region. Hatched areas show wind velocity (magnitude) greater than 10 ms^{-1}. Boxes in lower right hand corner of each figure provide the information for averaged area.

abruptly increased as on October 1 to the end of the next day (Figs. 6a, 6b), respectively. The box and whisker plots clearly show the shape of the distribution, central values and variability of the SLP and relative humidity values. Figure 7 indicates (a) time series of daily total precipitation in Bandar-e-Anzali station, where the highest value was observed and (b) areal average over 37°N during the study period. This type of event is kind of rare and potentially devastating over southern coasts of Caspian Sea. At landfall, wind speeds averaged over 10 ms^{-1} and 24-h rainfall total exceeded 220 mm (Figs. 7a, 7b). Based on Figure (7a), the life cycle of the storm was almost three days long over the region under study, but the peak of the storm activity occurred on October 1, 2001. Therefore, in this case

study, we mostly focus on the synoptic features of the event for this day. Geopotential heights together with relative vorticity are shown in Figs. 8a and 8b. Black contours indicate the geopotential height of the 500 hPa surface, in meter. Since low geopotential height (compared to other locations at the same latitude) indicates the presence of a storm or trough at mid-troposphere levels, it can be seen that at 0600 UTC October 1, 2001 there is a huge trough originated from high latitudes (around 72N) extending toward the lower latitudes (around 30°N) over the southern coasts of Caspian Sea provided a suitable condition for air rising resulting in a weather turbulence in the regions ahead including the study area, while the surrounding areas where a relatively high geopotential height is predominant with a ridge, the weather is
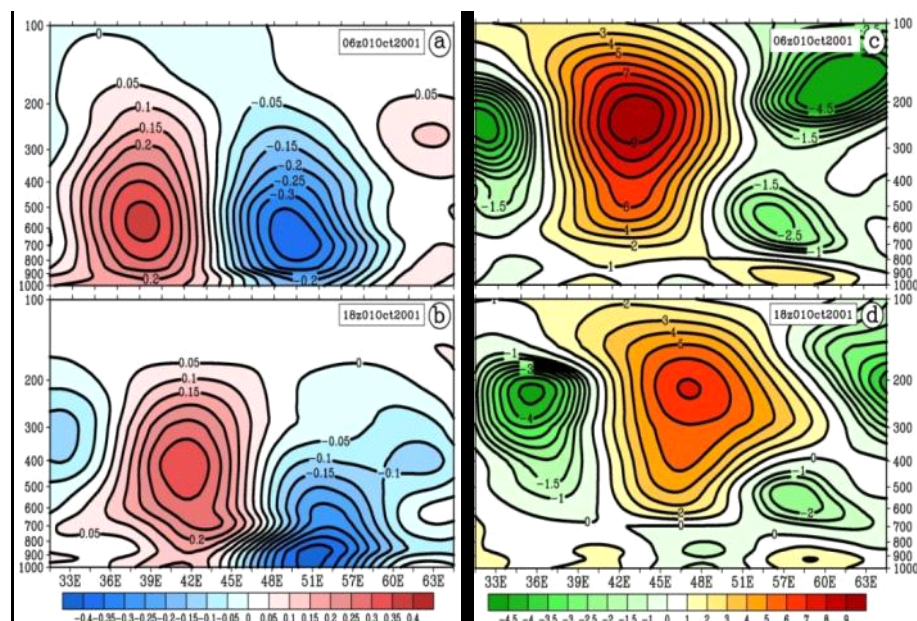
Fig. 11. The hourly cross-section of the vertical velocity (Pa s⁻¹) and relative vorticity (10⁻⁵ s⁻¹) along 37°N valid at: (a) and (c) 06 UTC, (b) and (d) 1800 UTC October 1, 2001.
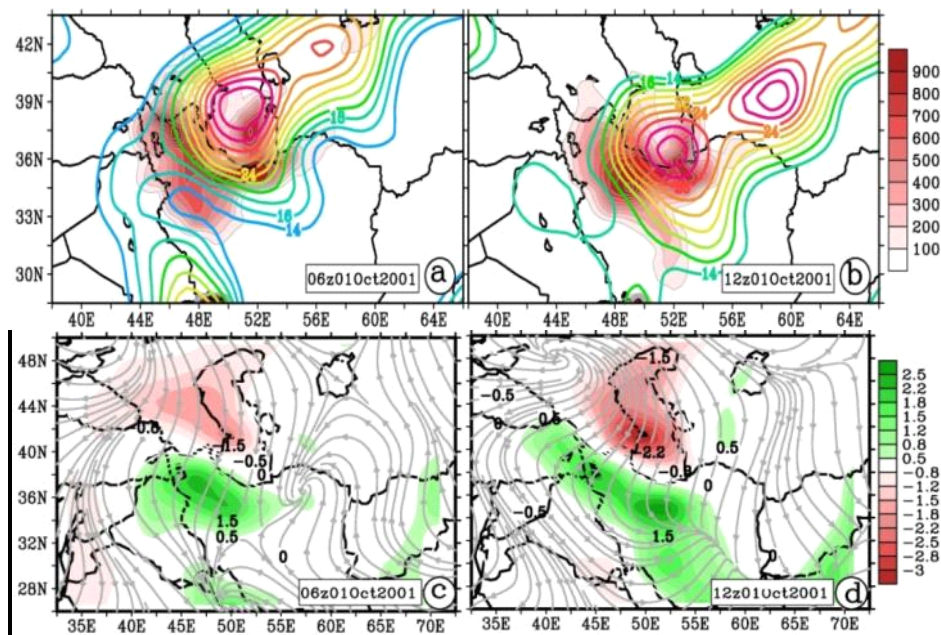
Fig. 12. The convective available potential energy (J kg⁻¹) shading and precipitable water (kg m⁻²) colorful contours valid at: (a) 0600 UTC (b) 1200 UTC of October 1, 2001. Moisture convergence (g kg⁻¹ s⁻¹) shading and wind (m s⁻¹) valid at: (c) 0600 UTC (d) 1200 UTC of October 1, 2001. All the figures are at surface level.

quiescent (Fig. 8a). The color shading indicates vorticity at 500 hPa: red for positive vorticity, blue for negative. Positive or cyclonic vorticity indicates counterclockwise rotation of the winds, and/or lateral shear of the wind with stronger flow to the right of the direction of flow, is quite strong exceeding 7x10⁻

⁵s⁻¹over the region. The positive vorticity is quite in good agreement with those of geopotential height fields, as positive vorticity at 500 hPa associated with cyclones or storms at upper levels and tend to coincide with troughs in the geopotential height field. 12-hours later, *i.e.* at 1800 UTC October 1, 2001, heights

contours increased to some extent and moved eastwards, as a result the storm's intensity slightly abated over the region (Fig. 8b), the system survived for the next day with less intensity (not shown). During the same period relative velocity (Fig. 8b) decreased compared to 12-h before, which observed less than $4 \times 10^{-5} s^{-1}$ over the study area. On October 1, 2001, a closed, surface high-pressure system had developed within a Westerly trough which was located in the northwestern side of Caspian Sea near 37°N-40°E. Figures 8c–f show the NCEP/NCAR derived SLP analyses at 0000 UTC, 0600 UTC, 1200 UTC and 1800 UTC October 1, 2001 respectively. During the 24-hours leading up to 1200 UTC October 1, the system was co-located below a cyclonic circulation in the apex of the mid to upper tropospheric trough. The trough was positively tilted and during 1800 UTC October 1 had started to retrogress towards the east coast of Caspian Sea. The surface high was located under a diffluent region at upper tropospheric levels, which helped maintain weak vertical wind shear above the system. The surface high moved eastward in accordance with the general easterly component of movement of the upper trough and also the northeasterly steering flow between the surface and the mid-troposphere circulation in the apex of the upper level trough. Hence, remaining within its diffluent, weakly sheared, large-scale environment the high pressure system slowly deepened as the upper level trough moved east, even though the upper tropospheric circulation appeared to weaken during 1800 UTC. From that time, the high accelerated northeast towards the east coasts of Caspian Sea (Fig. 8f). Hovmoller diagram of relative vorticity and SLP at longitude 49°E and latitude 37°N are shown in Figs. 9a and 6b, respectively. It clearly shows that a high pressure system with two-core closed centers had been active between latitudes 40°N and 50°N over the Caspian Sea (Fig. 9a). The high system had a central pressure of about 1014 hPa over latitude 48°N at 1200 UTC of September 30, when the first day of precipitation with less than 30 mm occurred. Within the next days, not only its central pressure intensified to more than 1026 hPa, but also extended much more towards the land led to the heaviest precipitation occurs over the southern coasts of Caspian Sea (Fig. 7a). The same variables are shown in Fig. 9b, from another angle (west to east of the region) at latitude 37°N. It can be seen that the negative relative vorticity (blue shading) varying between -0.5 and -3 covered the west of the region *i.e.* Bandar-e-Anzali and Rasht stations from late September to early October, while moved in a northeastward during the study period (Fig. 9b). This means that the severest precipitation occurred in the west of the study area i.e. Bandar-e-

Anzali (Fig. 7). The relative vorticity values are quite in good agreement with SLP contours as well as with those of wind velocities (hatched areas).

Figure 10 indicates the line graph of relative vorticity and SLP variables, which is compared in the land (solid line) and sea (dash line) over the region. It can be seen that the relative vorticity values are totally negative over the sea mainly on October 1, while it is almost positive over the land during the same period (Fig. 10a). Similarly, the SLP values increased dramatically at 0000 UTC of October 1, over the sea and slightly over the land (Fig. 10b). This is mainly because of locating the high system's eye over the Caspian Sea (Fig. 9). Therefore, the strong northerly wind began when the pressure difference between the Caspian Sea (sea) and north of Iran (land) increased to 8 hPa at 1200 UTC on October 1, which continued to more than 20 hPa until 0000 UTC on October 2, coinciding with the peak time of the system activity (Fig. 10).

Vertical velocity and Relative vorticity are other important parameters that we used to examine the severe storm under study. Figure 5 shows the hourly vertical velocity cross-section for October 1, 2001 along 37ÚN. An upward motion is seen along 47°-57°E, where the cyclone's core exists (Fig. 11a). The upward motion is drawn to the upper troposphere along 49°-52°N, where the cyclone was originated from. Therefore, strong upward motion (negative vertical velocity values) with more than -0.35 Pa s^{-1} is seen over the region at 0600 UTC of October 1 (Fig. 11a). 12-hours later at 1800 UTC of October 1, vertical velocity moved slightly eastwards, decreased to highly extent in values, and gradually the positive values (downward motion) were replaced on the study area (Fig. 11b). To understand the rotation and lateral shear of the winds within the storm vertically, the cross-sections of relative vorticity are examined for October 1, 2001. Examining the relative vorticity values along 37°N, it is seen that there is a strong cyclonic circulation between 700 and 200 hPa along 40°- 48°E. The values of positive vorticity varied between 3 and $9 \times 10^{-5} s^{-1}$ at 06 UTC of October 1, over the southern coasts of Caspian Sea (Fig 11c). While 12-hours later at 1800 UTC October 1, the positive vorticity in accordance with geopotential heights moved eastward (Fig. 11d), as a result the values greatly decreased to less than $6 \times 10^{-5} s^{-1}$ over the region. It is worthwhile to mention that there is also an increase in the negative vorticity values between 1000 and 800 hPa during the same period (Figs. 11d). We also tried to investigate the storm in relation to the precipitable water, CAPE value as well as moisture convergence condition (Fig. 12).The rainbow contours indicate total precipitable water in the atmosphere in October 1, 2001
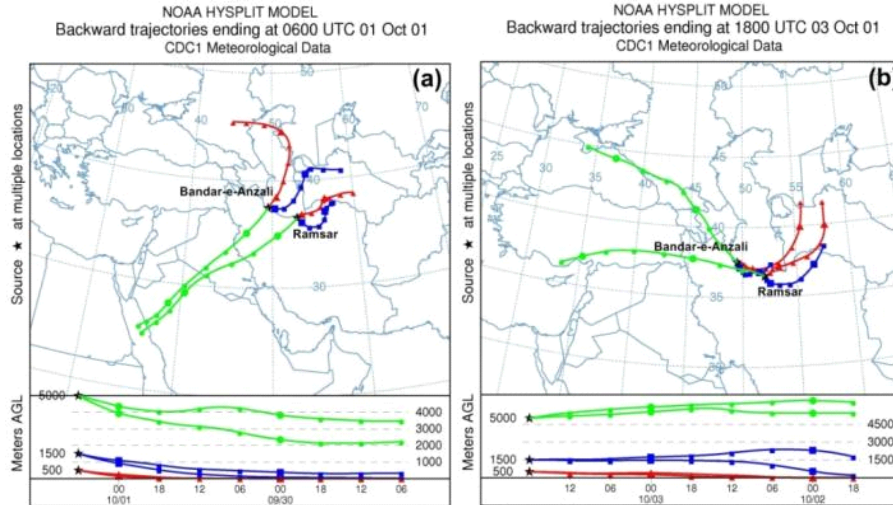
Fig. 13. HYSPLIT model backward trajectory outputs ending at the peak time (a) and ending time (b) of storm's activity over the region valid at 0600 UTC October 1, and 1800 UTC October 3, 2001 respectively. Model ran for 48 hours and used a 6 hour time steps (nodes). The figures demonstrate the individual air parcels at three levels (500, 1500 and 5000 m above ground level (AGL)) selected at Bandar-e-Anzali and Ramsar stations. Backward trajectory cross sections included in bottom of each figure for same levels.
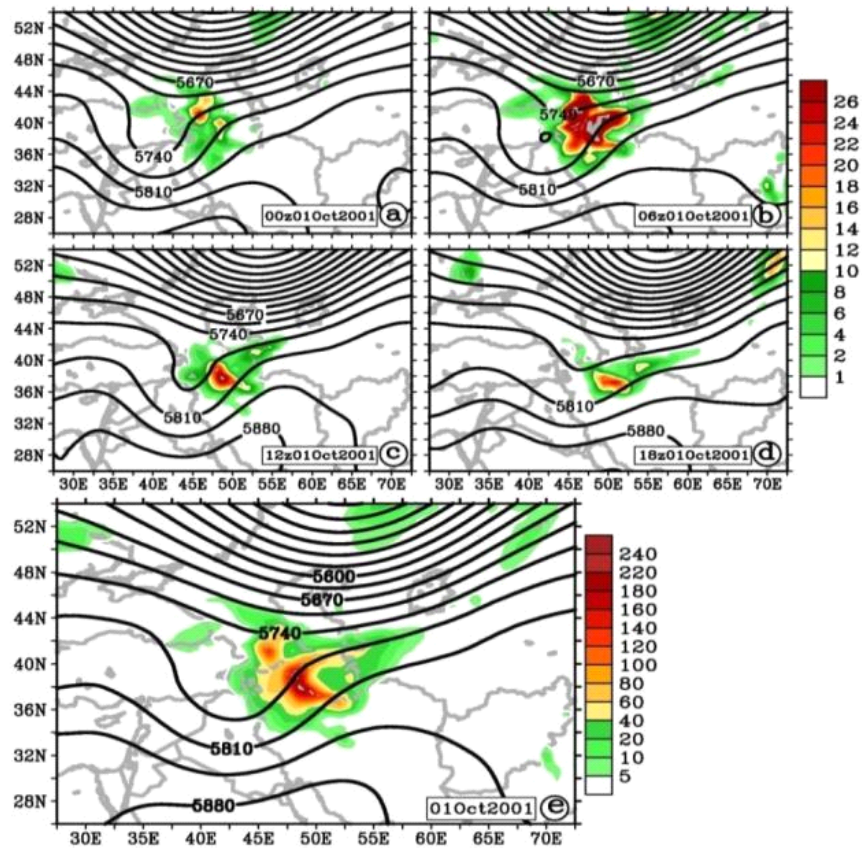
Fig. 14. Interim-full-daily total of precipitation (mm) data in 3-hours step derived from ECMWF and 4-times daily geopotential height (m) at 500 hPa derived from NCEP/NCAR reanalysis dataset valid for (a) 0000 UTC October 1, (b)) 0600 UTC October 1, (c)) 1200 UTC October 1, (d)) 1800 UTC October 1, 2001; and (e) daily total of precipitation and 500 hPa mean daily geopotential height valid for October 1, 2001.

(Figs 12a, 12b). Precipitable water, by definition, is the total depth of liquid water that would result if all water vapor contained in a vertical column of air could be "wrung out", leaving the air completely dry. It indicates the total humidity of the air above the region under study, and therefore, is a good indicator of the amount of moisture potentially available to supply rainfall (COLA, 2013). The amount of precipitable water exceeding 27 kg m^{-2} at 0600 UTC October 1 (Fig. 12a) and 26 kg m^{-2} at 1200 UTC of October 1, 2001 (Fig. 12b) over the southwestern parts of the Caspian Sea. The light pink to dark rose shading indicates the CAPE value in the atmosphere of the study area, which is a good indicator for the convective activity of the atmosphere, favorable for the formation of thunderstorm and other severe weather systems. The high values of CAPE indicate that one of the essential conditions for the thunderstorm exist for strong thunderstorms. It can be seen that the amount of CAPE exceeds 900 Jkg^{-1} over the region (Figs. 12a, 12b). Figures 12c, 12d, depict surface wind and moisture convergence. This chart is most useful for locating areas where thunderstorms likely to develop. The shading represents moisture convergence, green for convergence – positive areas, and red for divergence – negative areas, represented at a contour interval of 0.5 g/kg^{-1}s^{-1}. Areas of persistent moisture convergence over the southern coasts of Caspian Sea are favored regions for the storm development, since other factors *e.g.,* instability were quite favorable. Two of the primary factors in developing thunderstorms are a supply of moisture and low-level convergence. These two quantities are combined in these charts (Figs. 12c, 12d) to compute moisture convergence. Surface moisture convergence generally precedes the development of thunderstorms by a few hours. Generally, it is worthwhile to mention that there are good agreements both between the amount of the precipitable water and CAPE values (Figs. 12a, 12b), and moisture convergence and wind fields (Figs. 12c, 12d) during the study period over the southern coasts of Caspian Sea.

A backward trajectory Lagrangian model was also applied to detect of air parcels that came from far areas towards the given stations in order to tracking the moisture sources throughout the period of the severe storm under study. The model was run for two stations *i.e.* Bandar-e-Anzali and Ramsar with ending at the peak time and ending time of the storm's activity over the southern coasts of Caspian Sea at 0600 UTC October 1 (Fig. 13a), and 1800 UTC October 3, 2001(Fig. 13b) each one with 48 hours run duration. The result indicates that at the peak time of rainfall event *i.e.* at 0600 UTC October 1, 2001, due to the activity of an anticyclonic system over the Caspian Sea the air particles in the selected stations at lower levels *i.e.* 500 and 1500 meter above ground levels, originated mostly from Caspian Sea and the surrounding areas (Fig. 13a). It also clearly shows that the most amounts of rainfall occurred in Bandar-e-Anzali station (Fig. 7). At the same time, as a result of the deep trough over the region, the air particles at 5000 AGL came from southwest of Middle-East in particular from Red Sea (Fig. 13a). The backward trajectories with ending at end time *i.e.* 1800 UTC October 3, 2001for the storm (Fig. 13b) also indicate that the high system at surface level left the Caspian region completely eastwards resulted in to stop the moisture transport from Caspian Sea through lower levels streams i.e. 500 and 1500 AGL (Fig. 13b)., and air particles at 5000 AGL shifted its position from southwestern to a northwestern direction mainly due to the displacement of the deep trough toward east at 500 hPa level. The HYSPLIT model outputs confirm the synoptic features for the storm discussed above.

The daily total of precipitation data derived from ECMWF together with 4-times daily geopotential height at 500 hPa derived from NCEP/NCAR reanalysis dataset for October 1, 2001 are shown in Fig. 14. Figures 14a-14d, indicate hourly total of precipitation in 3-h steps for 0000 UTC October 1, 0600 UTC October 1, 1200 UTC October 1, and 1800 UTC October 1, 2001 respectively. While the hourly geopotential heights in 6-h steps overlaid for the same dates. According to the figures, in early October 1, the southwestern portion of the southern coasts of Caspian Sea were situated in front of a deep trough and due to availability of other criteria such as instability and moisture convergence, a considerable amount of rainfall recorded at 0000 UTC October 1 (Fig. 14a). But the heaviest hourly rain occurred 6-hours later *i.e.* at 0600 UTC October 1, when 500hPa trough more deepened and other criteria for the event were available, which intensified the landfall over the region (Fig. 14b). The spatial distribution of the precipitation pattern is similar to that noted in the pressure patterns (surface and upper levels in Figs. 8). In fact, the heavy rainfall event is due to a deep inland trough that extended from northwest of the country to Caspian region along the southern coasts of Caspian Sea in the north of Iran. A cyclonic circulation was noticed between the height 4-km and 5-km over the southwestern portion of Caspian Sea along the southern coasts, especially over the north Gilan province coasts, where Bandar-e-Anzali station located and the surrounding area (Figs. 14b). The storm's intensity let up for the coming hours, and moved eastward to some extent but went on to rain with less intensity over the study area (Figs. 14c, 14d). The daily total of precipitation together with 500 hPa

Table 3. Cyclone intensity scale over the southern coasts of Caspian Sea

Category	Type	Pressure (hPa)	Accumulated precipitation (mm)	Line color
1	Deep Depression	<1021	<120	Green
2	Cyclonic Storm	1022-1028	121-200	Blue
3	Sever Cyclonic Storm	1029-1035	201-250	Yellow
4	Very Sever Cyclonic Storm	1036-1042	251-300	Orange
5	Super Cyclonic Storm	>1043	>301	Red

Table 4. Frequency and percentage of cyclone events in individual categories

	Cyclone tracks in warm seasons						Cyclone tracks in cold seasons				
	Cat. 1	Cat. 2	Cat. 3	Cat. 4	Cat. 5		Cat. 1	Cat. 2	Cat. 3	Cat. 4	Cat. 5
Frequency	6	6	1	1	1	Frequency	10	18	8	2	4
Percentage	40%	40%	6.6%	6.6%	6.6%	Percentage	23.8%	42.9%	19%	4.8%	9.5%
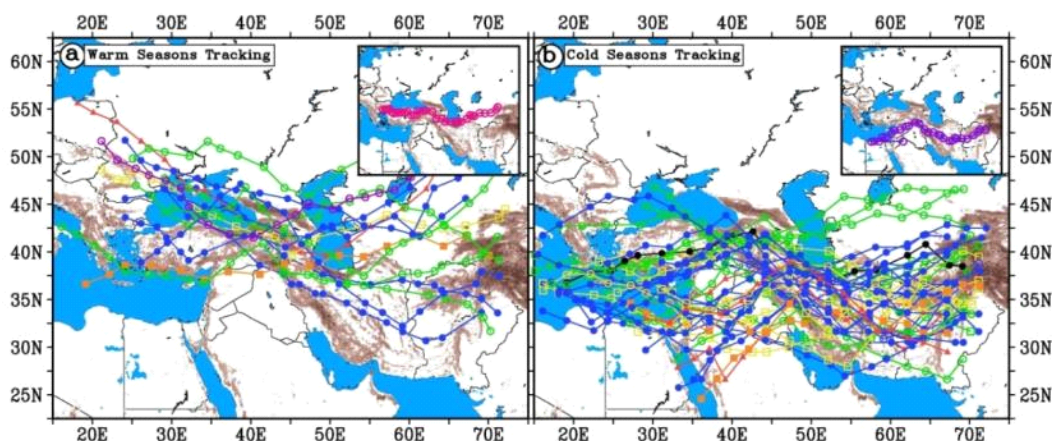
Fig. 15. Daily tracking of cyclones in (a) warm-months (15 tracks) from April to September and (b) in cold-months (42 tracks) from October to March, during a ten-year period: 1996-2005 over the southern coasts of Caspian Sea. All 57-tracks were classified into five categories based on table 1: Cat. 1: green trajectories with a closed circle marker; Cat. 2: blue trajectories with an open circle marker; Cat. 3: yellow trajectories with a closed square marker; Cat. 4: orange trajectories with an open square marker; and Cat. 5: red trajectories with a solid triangle marker. The subplots on the top right corner of each plot indicate the predominant (average) path of cyclones (a) in warm-seasons, and (b) in cold-seasons over the region. The black trajectory indicates the track of cyclone in October 2001, which was examined above as a case study.

mean daily geopotential height is shown in figure 11e. It is quite in a good agreement with those of the hourly total of precipitation discussed above. The position of maximum rainfall (220 mm) observed over Bandar-e-Anzali (37.3º N, 49. 2º E) is well-represented in the Figure 14e. The result (Fig. 14) of rainfall distribution along the southern coasts of Caspian Sea shows the presence of a large-scale cyclonic circulation at upper levels and anticyclonic circulation at surface leading to the heavy rainfall event over the southern coasts of

Caspian Sea. In the last part of the research it is aimed to investigate the frequency of cyclones and their tracking for warm-seasons and cold-seasons separately over the southern coasts of Caspian Sea. Therefore, 57 cyclones derived from table 1 are used to draw the climatology of cyclones tracking for a ten-year period from 1996 to 2005. First, we classified all 57 cyclones into five categories based on pressure (values of closed pressures around high over the Caspian Sea) and accumulated precipitation of the

selected stations in the region (Table 3). The daily track of 15 cyclones during warm-months with different intensities is shown in Fig. 15a. According to Table 4, most of the cyclones (80%) occur within the categories of 1 and 2 (table 4), as deep depression and cyclonic storm, respectively (Table 3), which indicates that, less significant storms have struck the region during the study period. In addition, it can be seen that Black sea has a great influence on either cyclogenesis or strengthening the cyclones passing through the Caspian region. Mediterranean Sea is also another important water body in this regard. Another fact is that, during the warm-months, the activities of cyclones are mostly observed between latitudes 35°N and 53°N. This is due to the fact that the *Sub-Tropical High Pressure* (STHP) is predominant around latitude 28°N in summer, and as a result track of cyclones are shifted to the higher latitudes to a large extent. Therefore, not only the frequency of the cyclones over Iran, compared to cold seasons, is considerably decreased, but also rainfall events in summer are mostly limited to the Caspian region (Fig. 15a).

As well as, the daily track of 42 cyclones during cold-months is shown in Fig. 15b. The highest frequency of cyclones, as table 4 indicates, occurs in the form of cyclonic storm with 18 tracks (42.9%) in category 2. The categories of 1 and 3 are ranked as second and third positions with 10 track (23.8%) and 8 tracks (19%), respectively. Interestingly, 4 super cyclonic storms also took place within a ten-year period over the Caspian region. As it can be seen from the map, activity of the cyclones is mainly observed between latitudes 28°N and 45°N during the cold-months. It is also worthwhile to mention that most cyclones over the region originated from Mediterranean Sea and Red Sea to some extent. Therefore, Mediterranean Sea plays a significant role in cyclogenesis and transferring them to the Caspian region (Fig. 15b). The subplots in each map, which indicate the predominant trajectory of cyclones, clearly show that the general path of cyclones have oscillation in approximately 5-10 degrees from cold seasons (dark purple trajectory) to warm seasons (magenta trajectory) mainly because of the predominancy of sub tropic high pressure over the south of Iran in summer periods.

CONCLUSIONS

A climatology of cyclonic systems affecting the southern coasts of Caspian Sea bounded by the area, north of 36°N, south of 38°N, west of 55°E and east of 48°E, based on the systems formed during 1996-2005 has been developed. The climatology includes severe cyclonic systems with at least one analyzed closed SLP contour in addition to rainfall falling within threshold criteria (above 50 mm) at selected coastal

observing stations. Stations located in the west of the Caspian region received the extreme rainfall during late summer and early autumn seasons. On the contrary, the eastern stations in the Caspian region received the severest rainfall during winter season. The number of cyclones formed over the west Caspian region is much more than those occurred in the eastern region as well as the most frequent cyclone event occurred in the year 1977 with 9 storms, while the lowest one took place in the year 1998 with only 2 storms. On the whole, the frequency of cyclone occurrence indicated a year-to-year fluctuation; nevertheless it showed a slightly ascending trend over the region. Time series of the accumulated precipitation of five stations, caused by 57 cyclone events, in cold was almost twice as that in warm season, which indicated that not only the frequency of cyclone events in the cold season (42) is far more than that in warm season (15), but also the intensity of storms is more in cold season over southern coasts of Caspian Sea.

Approximately 73.7% of the systems (42 out of 57), occurred from August through December months, and 26.3% of the systems (15 out of 57) took place from January through May over the entire Caspian region. As well as most cyclones occur within the categories of 1 and 2 with 16 (28%), and 24 (42.1%) as deep depressions and cyclonic storms, respectively. Meanwhile, during the cold seasons, 4 super cyclonic storms (classified as fifth category) also took place within a ten-year period over the Caspian region. Mid-tropospheric, large-scale processes and local features were responsible for the initial development of all systems. Generally, the quantity of precipitation in the eastern stations was less than one third of the amount in the western stations, which means that the total precipitation is decreased gradually from west to east in the Caspian region. During the warm-months, the daily tracks of cyclones were largely shifted to north Caspian Sea due to the predominance of sub tropic high pressure.

Therefore, not only the frequency of the cyclones over Iran, compared to cold seasons, was considerably decreased, but also rainfall events in summer were mostly limited to the Caspian region. On the whole, the Mediterranean Sea plays a significant role in cyclogenesis and transferring them to the Caspian region. The detailed synoptic analysis of the October 2001 high-pressure system over the Caspian Sea has been described. On the basis of the analysis of the system up to its landfall, we found that the average wind speed was more than 10 ms^{-1} and 24-h total rainfall exceeded 220 mm mainly in Bandar-e-Anzali station.

The positive vorticity, which exceeded $7 \times 10^{-5} s^{-1}$ over the region, was quite in a good agreement with those of geopotential height fields, as positive vorticity at 500 hPa is associated with cyclones or storms at upper levels, and tend to coincide with troughs in the geopotential height field. Hovmoller diagram of relative vorticity and SLP showed that a high pressure system with two-core closed centers had been active between latitudes 40°N and 50°N over the Caspian Sea. The line graph of relative vorticity and SLP variables indicated that the relative vorticity values were totally negative over the sea while it was almost positive over the land during the same period. Similarly, the SLP values increased dramatically over the sea and slightly over the land. As a result, a strong northerly wind began when the pressure difference between the Caspian Sea (sea) and north of Iran (land) increased. Furthermore, a strong upward motion (negative vertical velocity values) with more than -0.35 Pa s^{-1} was seen over the region during the examined period. And also examining the relative vorticity values along 37°N, it was seen that there was a strong cyclonic circulation between 700 and 200 hPa along 40°- 48°E. The values of positive vorticity varied between $3 \times 10^{-5} s^{-1}$ and $9 \times 10^{-5} s^{-1}$ the amount of CAPE exceeded 900 J/kg^{-1} over the southern coasts of Caspian Sea. Areas of persistent moisture convergence over the region were favored regions for the storm development, since other factors *e.g.,* instability were quite favorable. The amount of precipitable water varied between 27 kg/m^{-2} and 26 kg m^{-2} over the southwestern parts of the Caspian Sea. Generally, there were good agreements both between the amounts of the precipitable water and CAPE values as well as moisture convergence and wind fields during the study period over the southern coasts of Caspian Sea. The result of the backward trajectory Lagrangian model indicated that at the peak time of rainfall event *i.e.* at 0600 UTC October 1, 2001, due to the activity of an anticyclonic system over the Caspian Sea the air particles in the selected stations at lower levels *i.e.* 500 and 1500 meter above ground levels, originated mostly from Caspian Sea and the surrounding areas. Thus, the HYSPLIT model outputs confirmed the observed synoptic features for the system of October 2001discussed as case study.

REFERENCES
Afshar Moghadam, Y. (1994). Vorticity and Divergence Analysis over the Caspian Sea, Master's thesis in marine physics., Islamic Azad University, north-Tehran branch (In Persian).

Alijani B. (1993). Air rising mechanisms for rainfall in Iran, J. of the literature and humanities sciences faculty, University of Tarbiat Moalem, summer 1993, new version (1), 85-101pp (In Persian).

Alijani B. (1997). Climate of Iran, University of Payam-e-Nor publication, third edition, 221p (In Persian).

Alijani B., (2001). Weather types and their influences on Iranian climate., J. of research, 2 (3), 21-49pp (In Persian).

Alijani B., Mohammadi, H. and Bigdeli, A. (2007). The role of pressure patterns in the precipitations of the southern coasts of Caspian Sea, quarterly J. of Territory, forth year, 16, 37-51pp (In Persian).

Bagheri, S. (1993). Synoptic investigation of flooding systems in north of Iran., Master's thesis in meteorology, institute of geophysics, University of Tehran (In Persian).

Blender, R., K. Fraedrich, and Lunkeit, F. (1997). Identification of cyclone track regimes in North Atlantic. Quart. J. Roy. Meteor. Soc., **123**, 727–741.

Draxler, R.R. and Rolph, G. D. (2011). HYSPLIT (HYbrid Single-Particle Lagrangian Integrated Trajectory) Model access via NOAA ARL READY Website.

Ghashghaei, G. H. (1996). The investigation of Siberian high effect on the autumn precipitations over the southern coasts of Caspian Sea, Master's thesis in physical geography, University of Tarbiat Moalem (In Persian).

JanbazGhobadi, Gh., Mofidi, A. and Zarrin, A. (2001). Synoptic patterns identification of the wintertime severe precipitation over the southern coasts of Caspian Sea, J. of geography and environmental planning, **22 (2),** 23-4pp (In Persian).

Hobbs, P. V., Locatelli, J. D. and Martin, J. E. (1990). Cold fronts aloft and the forecasting of precipitation and severe weather east of the Rocky Mountains. Wea. Forecasting, 5, 613–626.

Hobbs, P. V., Locatelli, J. D. and Martin, J. E. (1996). A new conceptual model for cyclones generated in the lee of the Rocky Mountains. Bull. Amer. Meteor. Soc., **77**, 1169–1178.

Kalnay, E., Kanamitsu, M., Kistler, R., Collins, W., Deaven, D., Gandin, L., Iredell, M., Saha, S., White, G., Woollen, J., Zhu, Y., Leetmaa, A., Reynolds, R., Chelliah, M., Ebisuzaki, W., Higgins, W., Janowiak, J., Mo, K.C., Ropelewski, C., Wang, J., Jenne, R. and Joseph, D. (1996). The NCEP/ NCAR 40-year reanalysis project, Bull. Amr. Met. Soc., **77**, 437-471.

Key, J. and Chan, A. (1999). Multidecadal global and regional trends in 1000 mb and 500 mb cyclone frequencies. Geophys. Res. Lett., **26**, 2053–2056.

Khalili, A. (1971). The origination of rainfalls over the southern coasts of Caspian Sea, J. of Nivar, 1971, 39-4 (In Persian).

Khoshhal, J. (1997). Analysis of the models of climatology for precipitations more than 100mm over the southern coasts of Caspian Sea., PhD thesis in physical geography, University of Tarbiat Modares (In Persian).

Moradi, H., (2001). Synoptic investigation of flood on November 11th 1996 in the central parts of Mazanderan province., J. of Training Growth of Geography, **57**, 33-41 (In Persian).

Moradi, H., (2004). The role of Caspian Sea in the precipitation of northern coasts of Iran, J. of marine technics and sciences of Iran, second periods (2-3), 77-88 (In Persian).

Moradi, H. (2006). Flooding occurrence prediction based on synoptically situations over the southern coasts of Caspian Sea, J. of geographic researches, NO. 55, 109-131 (In Persian).

PourAtashi, M. (2005). Synoptic study of the heavy precipitation (more than 200mm in a 24-h duration) resulting from the heat advection at the middle layers of the atmosphere over the southern coasts of Caspian Sea, Master's thesis in meteorology, Islamic Azad University, North-Tehran branch (In Persian).

Raziei, T., Mofidi, A. and Zarrin, A. (2008). Activity centers and the circulation patterns of wintertime atmosphere at 500 hPa over the Mideast and their relations with Iranian precipitation, J. of earth and space physics, **35 (1)**, 121-141 (In Persian).

Rolph, G. D. (2011). Real-time Environmental Applications and Display sYstem (READY) Website, NOAA Air Resources Laboratory, Silver Spring, MD

Rossby, C. G. and R. H. Weightman, (1926). Application of the polar front theory to a series of American weather maps. Mon. Wea. Rev., **54**, 485–496.

Sanders Donald, H. (2001). Statistics: A First Course. First Canadian Edition. Whitby, Ontario: McGraw-Hill Ryerson.

Serreze M. C., Box R. G. and Walsh J. E. (1993). Characteristics of Arctic Synoptic Activity, 1952-1989. Meteorol. Atmos. Phys., **51**, 147–164.

Serreze, M. C. (1995). Climatological aspects of cyclone development and decay in the Arctic. Atmos.–Ocean, 33, 1–23.

Serreze, M. C., F. Carse, R. G. Barry, and J. C. Rogers, (1997). Icelandic low cyclone activity: Climatological features, linkages with the NAO, and relationships with recent changes in the Northern Hemisphere circulation. J. Climate, **10**, 453–464.

Stunder, B. J. B. (1997). NCEP Model Output – FNL ARCHIVE DATA, TD-6141. Prepared for National Climatic Data Center (NCDC).

Taljaard J.J. (1967). Development, distribution and movement of cyclones and anticyclones in the Southern Hemisphere during the IGY. J. Appl. Met., **6**, 973–987.

Trigo I. F., Davies T. D., and Bigg G. R. (1999). Objective climatology of cyclones in the Mediterranean region. J. Climate, **12**, 1685–1696.

Vahidi, J. (1997). Statistical-synoptic investigations of the rainfall over the southern coasts of Caspian Sea, Master's thesis in meteorology, Islamic Azad University, North-Tehran branch (In Persian).

Whittaker, L. M. and Horn, L. H. (1981). Geographical and seasonal distribution of North American cyclogenesis,. Mon. Wea. Rev., **109**, 2312–2322.

Yousefi, H. (2003). Arrival scheduling of the Siberian high to the southern coasts of Caspian Sea and its effect on the autumn precipitation of the region, Master's thesis in physical geography-climatology, faculty of geography, University of Tehran (In Persian).

Yatagai A., Arakaw O., Kamiguch A., Kawamoto K., Nodzu H. and Hamada M. I. (2009). A 44-year daily gridded precipitation dataset for Asia based on a dense network of rain gauges, SOLA, **5**, 137-140.

Zishka, K. M. and Smith, P. J. (1980). The climatology of cyclones and anticyclones over North America and surrounding ocean environs for January and July, 1950–77. Mon. Wea. Rev., **108**, 387–401.